Energy, Exergy, and Economic Analyses of a Combined Heat and Power Generation System with a Gas Turbine and a Horizontal Axis Wind Turbine

Ajam, Mohammad; Mohammadiun, Hamid*[+]; Dibaee Bonab, Mohammad Hossein*[+]; Mohammadiun, Mohammad

Department of Mechanical Engineering, Shahrood Branch, Islamic Azad University, Shahrood, I.R. IRAN

ABSTRACT: *Using the Combined Heat and Power (CHP) systems is known as one of the most effective ways to raise the power coefficient and reduce fuel consumption and operational costs. In this study, a CHP system with the prime movers of a gas turbine and a horizontal axis wind turbine under the strategy of providing electric charge has been investigated based on the first and second laws of thermodynamics. This study aims to evaluate the effect of a wind turbine on the CHP system. The results show that the proposed CHP system has significant advantages compared to the CHP system working without the wind turbine. The best operating condition for the wind turbine is at the wind speed of 12 m/s, a pitch angle of 5^{o,} and a tip speed ratio of 3. Moreover, the effects of the wind speed and tip speed ratio on the exergy efficiency of the total system become considerable when the gas turbine works at high-pressure ratios (more than 10) and the combustion chamber temperature is below 1250 ^{o}C. Also, it is shown this integrated system can reduce operational costs and fuel consumption by 55 % and 60%, respectively. Finally, regarding the interest rate, the payback period will be equal to 5.4 years.*

KEYWORDS: *CHP system; Gas turbine; Wind turbine; Exergy analysis.*

INTRODUCTION

environmental pollution and energy resource reduction have been the most important issues in recent decades [1,2]. Therefore, it is needed to adopt new strategies for the power coefficient improvement to decrease fuel consumption, and pollution of traditional energy conversion systems.

CHP systems can be a good solution for these issues as they increase energy and exergy efficiencies, and reduces fuel consumption and environmental pollutants by using dissipated heat from the prime mover [3–5]. In addition, Renewable energy resources such as wind and solar have been considered as the resources that have met the energy demand without any environmental pollution [6,7]. Therefore, the combination of CHP systems and renewable energy systems which can boost the overall efficiency of an integrated system has become a popular topic among researchers to address the energy crises [8,9]. In this study, we will evaluate a CHP system containing a gas turbine and a wind turbine as the prime movers in different conditions to increase productivity and decrease fuel

* *To whom correspondence should be addressed.*
+ E-mail: hmohammadiun@iau-shahrood.ac.ir ; diba_mr60@yahoo.com
1021-9986/2022/6/2100-2120 21/$/7.01

consumption based on the first and second laws of thermodynamics.

Recent studies

Several studies have been conducted to assess the CHP system's performance aimed to choose an optimum condition where the system has the highest heat and power output with the lowest intake of fuel and pollution. Nouri Proposed and simulated a new system of combined heat and power with the Brighton cycle as the main unit of electricity generation using renewable energy systems for residential districts[10]. Jamalabadi examined a hybrid system including a fuel cell module and a small-scale gas turbine based on the energy and exergy efficiency aimed to choose an optimal compressor pressure ratio to minimize carbon dioxide emission [11]. Also, in another study, Jamalabadi presented a mobile heat and power system for residential users with improved CO_2 reduction and examined it by the first and second laws of thermodynamics. The system includes a fuel cell power module, compressor, interrogator, a mini-gas turbine, and a circulating fluidized bed to absorb carbon dioxide [12].

Bagherzadeh suggested that the use of compressed air and an organic ranking cycle improve the performance of a Brighton power cycle [13]. Moreover, the optimal operating conditions for the compression ratio of each cycle were examined based on the first and second law of thermodynamics. Their results showed that the optimal compression ratio for all organic liquids is 5.5 and the optimal pressure ratio of the organic renin cycle for isopentane and n-pentane is 5.5 Isopentane has the least exergy damage, while the maximum efficiency of the first and second rules is achieved by R123. Acar and Arslan presented energy and exergy analysis of the organic resin cycle with solar energy and geothermal energy. Their results show that the energy output of the proposed system will be around 305 to 713 kWh [14]. These studies showed how a combined energy system can increase overall productivity. However, it is needed to study more about the effect of some important parameters on the output performance of the systems.

One parameter that has an important effect on the output power is fuel. Several studies related to the effects of various fuels on the gas turbine's performance as the prime mover of CHP systems are conducted [15]. *Ayala* studied the effects of using several types of natural gas, diesel, ethanol, and biofuels in gas turbines [16]. *Cavazre* also analyzed a gas microturbine with a combination of various types of organic and diesel fuels [17]. They studied the effects of different inlet fuels on the performance of the gas turbine and the emission of pollutants. *Yucer* examined a small-scale gas turbine jet engine in four different types of loads [18]. He examined the performance of the gas turbine in standby mode, full load, and two minor load modes, in terms of energy and exergy. His target parameters included energy consumption, fuel intake reduction, reduction of exergy degradation, relative exergy consumption, and exergy improvement.

One important tool to evaluate renewable and hybrid systems is the second law of thermodynamics [16–18]. It not only can depict the effects of each parameter on the system but also be able to evaluate the system economically[21–23]. Merve studied a solar- and geothermal energy-powered Organic Rankine Cycle based on the first and second laws of thermodynamics and showed that though the total power extracted by the solar system is increased, energy and exergy efficiencies of the geothermal-powered ORC decreased [14]. In addition, *Lee* examined a new approach to improve the performance of micro-gas turbines [24]. Exergy analysis showed that the combustion chamber and solar collector had the highest rate of exergy destruction. The results of the economic analysis also shows that the repayment period of this system is less than 4 years, which makes this proposed system economically feasible.

On the other hand, numerous studies associated with wind energy implementation in an energy system have been done. They have shown how much presenting a wind turbine can improve the performance of a hybrid system. *Koroneos* studied the exergy efficiency of a renewable energy system including a wind turbine to determine the electricity production of a hybrid system [17]. It shows that wind flow has a dominant effect on energy and exergy efficiencies. Khosravi defined and assessed an off-grid hydrogen storage system combining solar panels and wind turbines, a hydrogen production unit, and a fuel cell. It was demonstrated that the average energy and exergy efficiencies of the wind turbine were 32% and 25%, respectively [21]. *Khalilzadeh* employed the exergy and thermoeconomic concept to assess using waste heat from a wind turbine for a desalination process [22]. It was shown that this idea seems to be useful as it increases

the exergy efficiency of the integrated system by 7.34%. Also, the average rate of return and payback period are predicted as 6.76% and 6.33 years, respectively.

Similarly, some studies focused on using the wind turbine in a CHP system. Nematollahi proposed a novel method to use the heat waste of wind turbines in an organic Rankine cycles system and analyzed it based on the second law of thermodynamic [23]. *Mohammadi* analyzed the exergy efficiency of a combined cooling, heating, and power system integrated with a wind turbine and compressed air energy storage system [24]. The result of this study revealed that wind turbines and combustion chambers are the most important sources of exergy destruction in this system.

All studies showed the importance of using wind turbines in a system, but they mostly assumed that the wind turbine works under stable operating conditions and the effects of changing some parameters of a wind turbine on the system were not studied.

Khanjari showed how metrological variables can change the exergy efficiency of a wind turbine [25,26]. He used Blade Element Momentum (BEM) theory to model a wind turbine, which is a numerical method of modeling the wind turbine with a satisfactory result. He concluded that besides changing the wind speed, which has the dominant effect on changing the exergy efficiency of a wind turbine, the effects of other metrological variables like temperature, pressure changes, and relative humidity are not negligible. These studies just evaluated the effect of metrological parameters on a single wind turbine working in a wind tunnel section. So, studying the effect of input variables of the wind turbine as a part of the CHP system on the overall performance of the system can be an attractive idea.

In this study, the BEM method will be used to model a horizontal axis wind turbine in a CHP system including a gas turbine as the prime mover and a wind turbine. The aim of this study is to evaluate the effects of the different operational conditions of a wind turbine on the performance of the described system and the energy and exergy efficiencies and finally assess this system economically in the best operating condition.

EXPERIMENTAL SECTION

Case study

Fig. 1 shows the CHP system which includes a gas turbine and a wind turbine. The gas turbine as a prime mover burns the fuel purchased from the global gas grid and generates electricity. Moreover, the wind turbine provides the other part of the electricity demand. If the electricity generated by these generators is still less than the building needs, the required electricity will be purchased from the global grid.

On the other hand, the heat output of the gas turbine will be recycled to supply the building's thermal loads. This recycled heat is used as a heat source to meet the heating load in winter or the hot water consumption during the year. If the recycled heat is less than the building's heating demand, the heating load will be provided by the auxiliary boiler.

The technical specifications of the gas turbine and wind turbine are given in Table 1.

Energy analyses

In the first step of designing the power generation system, the desired system should be adapted to the rules and principles of thermodynamics. Due to the combination of the CHP system with two different types of generators as the prime movers, energy analysis must be applied to the system. The purpose of these calculations is to determine the best condition with the highest output power, recycled heat, overall efficiency, and lowest fuel consumption.

Gas turbine energy analysis

the first law of thermodynamics is applied to the gas turbine as the prime mover. Thus Eq.1 can be used to calculate the energy conversion and by using Eqs. (2) and (3), the pressure ratio and air temperature after compressor compression can be obtained. Finally, the work consumed by the compressor is obtained from Eq. (4) [18,29,30].

$$\dot{Q} - \dot{W} = \Delta \dot{E} \tag{1}$$

$$\frac{P_2}{P_1} = r_p \tag{2}$$

$$\frac{T_2}{T_1} = \left(r_p\right)^{\frac{k-1}{k}} \tag{3}$$

$$\dot{W}_{Com} = \dot{m}_{air} \times \left[h_2 - h_1\right] = \dot{m}_{air}\left(C_{P,2} \times T_2 - C_{P,1} \times T_1\right) \tag{4}$$

In Eq. (4), $\dot{m}_{air}$ is the air mass flow rate in the compressor. The input heat of the gas turbine cycle

Table 1: Technical specifications of the gas turbine and wind turbine [27] and [28].

Technical specification	Wind turbine	Gas turbine
Nominal capacity (kW)	150 KW	2000 KW
Type of fuel	Renewable energy	Natural gas
Fuel consumption	-	520 m3/h

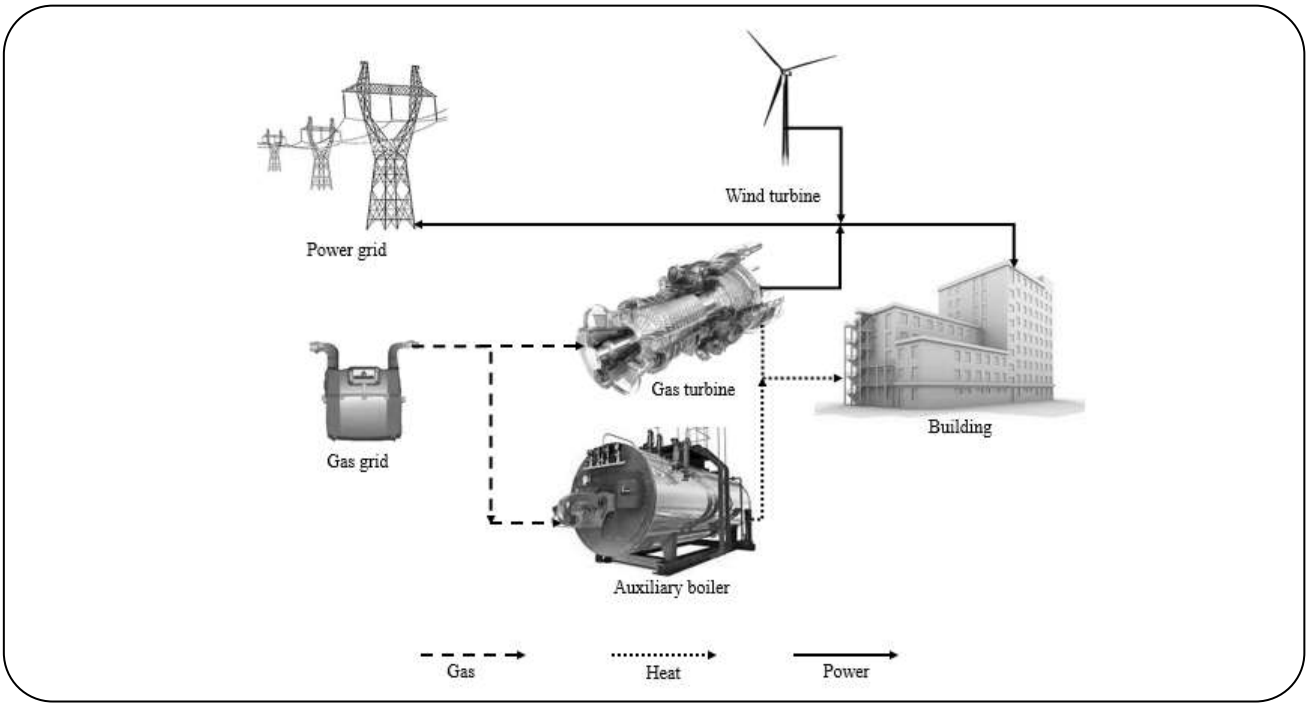

Fig. 1: CHP system combination.

Is provided through the combustion process in the combustion chamber, which is in accordance with Eq. (5). The mass flow rate of the gas turbine is equal to the total mass flow of the incoming air through the compressor and the inlet fuel in the combustion chamber and is obtained from Eq. (6). Finally, the power generated by the gas turbine is obtained from Eq. (7) [18,29,31].

$$\dot{Q} = \eta_{cch} \times \dot{m}_{fuel} \times LHV \quad (5)$$

$$\dot{m}_g = \dot{m}_{air} + \dot{m}_{fuel} \quad (6)$$

$$\dot{W}_{Tur} = \dot{m}_{gas} \times \left[h_3 - h_4\right] = \dot{m}_{gas}\left(C_{P,3} \times T_3 - C_{P,4} \times T_4\right) \quad (7)$$

Eqs. (8) and (9) show the rate of pressure drop at the inlet compressor and combustion chamber, respectively [29].

$$\Delta P_{air\,intake} = 0.008 P_{atm} \quad (8)$$

$$\Delta P_{CCH} = 0.01 P_2 \quad (9)$$

The efficiency of the turbine can be obtained by using the ratio of the output power to the heat generated through the combustion chamber. In addition, the efficiency of the gas turbine at any partial load can be estimated using Eq. (10) and based on the coefficient of nominal efficiency. The fuel consumption and recyclable heat from the gas turbine exhaust in partial loads can also be calculated from Eqs. (11) and (12), respectively [18,32].

$$\frac{\eta_{th,PL}}{\eta_{th,nom}} = -2.551 \times 10^{-5} PL^2 + 0.01135 PL + 0.1171 \quad (10)$$

$$\frac{\eta_{f,PL}}{\eta_{f,nom}} = -0.4772 \exp\left(0.007565 PL\right) - 0.2123 \exp\left(-0.02677 PL\right) \quad (11)$$

$$\frac{H_{ex,PL}}{m_{f,PL}LHV_{gas}} = 0.0061PL + 0.3868 \quad (12)$$

In Eqs. (10) to (12), *PL* indicates the percentage of partial load in the prime mover.

In Eq. (5), m_f indicates the amount of fuel consumption in the gas turbine at full load to reach the combustion temperature. This parameter (the first fuel consumption of the engine) will also change if the combustion chamber temperature, pressure ratio, altitude, and ambient temperature change. The fuel consumption can then be calculated based on Eq. (13) [29].

$$\dot{m}_{fuel} = \frac{\dot{m}_{gas} \times C_P \times (T_{out} - T_{in})}{LHV} \quad (13)$$

T_{in} in Eq. (13) is the inlet temperature of the combustion chamber, which is proportional to the gas turbine pressure ratio and is obtained by Eq. (3) with the specified turbine pressure ratio. In this equation, T_{in} is the ambient temperature and rp is the compression ratio in the gas turbine cycle. Also, the constant k of gas is ideal and is considered equal to 1.4.

By reducing the capacity of the equipment, the efficiency and performance coefficient are reduced compared to the nominal load. The operation of the boiler, like other equipment, is a function of the partial load value that can be calculated from Eq. (14).

Boiler:

$$\frac{\eta_{th,PL}}{\eta_{th,nom}} = 0.0951 + 1.525PL - 0.6249PL^2 \quad (14)$$

Exergy is a thermodynamic analysis of energy quality. Therefore, exergy can be defined as the maximum theoretical work that can be obtained from a system [33,34].

To determine the inefficiency of the system, the second law of thermodynamics is applied. It can help us calculate the inefficiencies and exergy destruction in each part [35,36].

The environmental condition is defined as the dead state [35].

To calculate the exergy, the equilibrium state of the system is considered. Therefore, the exergy of control volume in a stable state can be defined as Eq. (15) [34]:

$$\sum_j \left(1 - \frac{T_0}{T_j}\right)\dot{Q}_j - \dot{W}_{CV} + \sum_i \dot{m}_i ex_i - \sum_e \dot{m}_e ex_e - \dot{E}x_d = 0 \quad (15)$$

In Eq. (15), *T* is temperature, *ex* is exergy per unit mass, $\dot{Q}_j$ is heat transfer rate, $\dot{W}_{CV}$ is the work rate done by control volume and $\dot{E}x_d$ indicates the amount of exergy degradation. Also, below the gear *j* shows the equipment number, 0 indicates the state of the environment, i is the input current and *e* the output current.

Physical exergy in any mass flow is defined in a particular situation relative to the relational environment (16):

$$ex_{ph} = (h - h_0) - T_0(s - s_0) + \left(\frac{V^2 - V_0^2}{2}\right) + g(Z - Z_0) \quad (16)$$

In Eq. (16), *h, s, v, g,* and *z* represent the specific enthalpy, the specific entropy, the velocity, the gravity coefficient, and the height, respectively. In this study, due to the low speed and altitude values, these two parameters have been omitted [34].

The number of entropy changes can also be calculated using Eq. (17):

$$S_{out} - S_{in} = C_{p,ave} \times \ln\frac{T_{out}}{T_{in}} - R \times \ln\frac{P_{out}}{P_{in}} \quad (17)$$

On the other hand, the chemical exergy of a single gas in a mixture of several gases is calculated according to Eq. (18) [18]

$$\overline{ex}_i^{ch} = x_i \overline{ex}_i^{ch,0} + RT_0 x_i \ln(x_i) \quad (18)$$

In Eq. (18), *x* is the monolithic concentration of a gas. Also $\overline{ex}_i^{ch,0}$ is the standard one-way exergy extracted from sources [34,37] given in Table 2.

In a CHP system, the exergy efficiency is defined according to Eq. (19) [34,38,39]:

$$\eta_{ex,CHP} = \frac{\dot{W}_{net} + \left(1 - \frac{T_{amb}}{T_{Heat}}\right)\dot{Q}_{heat}}{\dot{E}x_f} \quad (19)$$

In Eq. (19), $\eta_{ex,CHP}$ is the exergy efficiency of the CHP system and $\dot{W}_{net}$ is the output of the net power of the simultaneous production system. T_{heat} is the average temperature of heat transfer. In addition, $\dot{E}x_f$ is the amount of fuel exergy which is obtained from Eq. (20) [40]:

$$\dot{E}x_f = \dot{m}_f \times ex_f \quad (20)$$

Table 2: Standard chemical exergy of different gas species [34, 37].

Type of the gas	Value	Unit
$\overline{ex}^{ch,0}_{H_2O}$	9.5	kJ/mol
$\overline{ex}^{ch,0}_{O_2}$	3.97	kJ/mol
$\overline{ex}^{ch,0}_{N_2}$	0.72	kJ/mol
$\overline{ex}^{ch,0}_{CO_2}$	19.87	kJ/mol

In Eq. (20), ex_f is a specific chemical exergy of fuel and is obtained from Eq. (21) [40].

$$ex_f = \varphi \times LHV \quad (21)$$

The parameter φ for natural gas is considered to be 1.04 [40].

The amount of exergy destruction per each piece of equipment is also calculated from Eq. (22) and k is the equipment counter [35]:

$$\dot{E}x_{d,k} = \dot{E}x_{i,k} - \dot{E}x_{e,k} \quad (22)$$

Wind turbine energy and exergy analysis

The energy efficiency(η) in Eq. (23) is the proportion of output power extracted from the wind turbine per the kinetic energy changes of wind flow before and after touching the wind turbine, while the exergy efficiency(Ψ) (Eq (24)) is the ratio of the power produced to the exergy changes of the wind (see Fig. 2).

$$\eta = \frac{W_{out}}{\text{kinetic energy changes}} \quad (23)$$

$$\Psi = \frac{W_{out}}{Ex_{flow}} \quad (24)$$

The kinetic energy changes can be defined by:

$$ke_1 = W_{out} + ke_2 \quad (25)$$

Where $ke_{1,2}$ is the inlet and outlet kinetic, respectively.

$$kx_{1,2} = \frac{1}{2}\dot{m}v_{1,2}^2 \quad (26)$$

The mass flow rate passing throughout the wind turbine is:

$$\dot{m} = \rho \pi r^2 v \quad (27)$$

The exergy flow is the summation of kinetic energy and physical exergy:

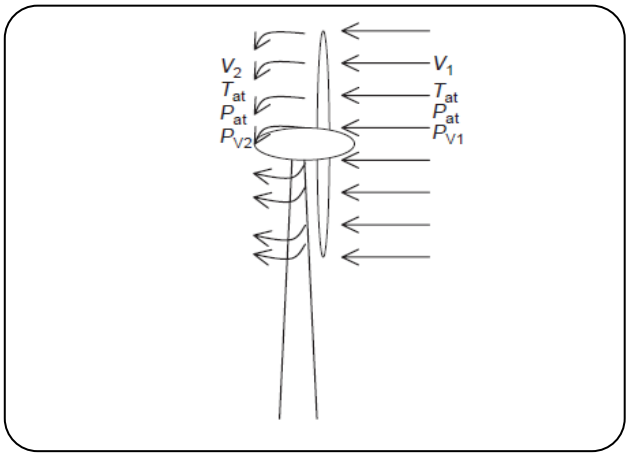

Fig. 2: Inlet and outlet variables in the wind system.

$$Ex_{flow} = Ex_{ph} + ke \quad (28)$$

$$Ex_{ph} = m\left[c_p\left(T_2 - T_1\right) + T_0\left(C_P \ln\left(\frac{T_2}{T_1}\right) - R\ln\left(\frac{P_2}{P_1}\right) - \frac{C_P\left(T_0 - T_{avg}\right)}{T_0}\right)\right] \quad (29)$$

Where $P_{1,2} = P_0 \pm (\rho/2)(V_{1,2})^2$. Also, the temperatures of flow in both states $T_{1,2}$ are calculated through the wind chill temperature formula developed in [41].

In this research, the reference pressure and temperature were assumed (101.3 kPa and 298 K), respectively.

BEM theory

Another prime mover is a horizontal-axis wind turbine. In this study, we will model a horizontal axis wind turbine based on the Blade Element Momentum (BEM) and calculate the energy and exergy efficiency of the wind turbine in different scenarios to measure the effect of the wind turbine on the overall efficiency of the system.

There are several ways to model a wind turbine to measure power output and efficiency. It can be model

by Computational Fluid Dynamics (CFD) tools based on the fully direct modeling, actuator line, disc, and surface methods [42–44]. Even though these methods have an acceptable output, they are very time-consuming and need a powerful computational system to solve the Navier-Stokes equations. Also, we can implement the BEM method to model a wind turbine. Compared to CFD models, this method needs less time to calculate the loads and the output results have a satisfactory prediction in most cases [26,45,46].

o have a better understanding of the BEM concept, it is assumed that the wind flow is incompressible and axisymmetric [47]. In this study, we used the BEM model developed by Glauert and Hansen [47,48].

Rotating the win blade in each angular velocity causes the wake behind the wind turbine, which can affect the upstream flow before touching the wind turbine [26]. Consequently, V_1 is the wind speed before touching the wind turbine and it will be declined by the wake-induced velocity [47].

$$V_1 = V_0(1-a) \tag{30}$$

That *a* is the axial induction factor.

To avoid the breaking down of the integration process, a correction variable must be used as Eq. (31) [49,50].

$$a= \begin{cases} (k+1)^{-1}, & a \le a_c \\ \frac{1}{2}(2+k(1-2a_c)-\sqrt{(k(1-2a_c)+2)^2+4(k.a_c{}^2-1)}), & a \ge a_c \end{cases} \tag{31}$$

$$k = \frac{4f\sin\phi^2}{\sigma'(c_1\cos(\phi)+c_d\sin(\phi))} \tag{32}$$

$$\sigma' = 3c/2\pi r \tag{33}$$

Where *k* is an auxiliary function and a_c = 0.3 is the separation point of the thrust coefficient in the high axial induction factor, C_l and C_d are the lift and drag coefficients.

Also, the tip loss correction used in this study can be defined by [47]:

$$f = \frac{2}{\pi}\arccos\left(e^{-\left(\frac{3(R-r)}{2r\sin\phi}\right)}\right) \tag{34}$$

f is Prandtl's tip loss correction of the turbine as a finite-bladed rotor.

Moreover, there is a similar equation for the rotational speed[51,52].

$$a' = \frac{w_{i2}}{\Omega} \tag{35}$$

Where w_{i2} is the tangential induced velocity at the plane just before the rotor and $\acute{a}$ is the tangential induction factor.

Other parameters like the angle of flow (ϕ) and the angle of attack (α) are followed by Eqs. (36) and (37).

$$\phi = a\tan\left(\frac{V_0(1-a)}{r\Omega(1+a')}\right) \tag{36}$$

$$\alpha = \phi - \beta \tag{37}$$

Regarding Fig. 3, to calculate the power produced by a wind turbine, the axial and tangential forces on a blade element should be calculated:

In Fig. 3, V_o is incoming wind speed, Ω is the angular velocity of the blade, r is the local radius of the element, *W* is relative velocity, β is pitch angle, ϕ is flow angle, *L* and D are the induced lift and drag forces per blade length, respectively [47].

$$W = \sqrt{V_o^2(1-a)^2+\Omega^2r^2(1+a')^2} \tag{38}$$

$$L = \frac{1}{2}\rho W^2 C_l c \quad , \quad C_l = f(r,\alpha) \tag{39}$$

$$D = \frac{1}{2}\rho W^2 C_d c \quad , \quad C_d = g(r,\alpha) \tag{40}$$

$$dF_{ax} = L.\cos(\phi)+D.\sin(\phi) \tag{41}$$

$$dF_{tan} = L.\sin(\phi)-D.\cos(\phi) \tag{42}$$

$$Power = \Omega\int_{r_{hub}}^{R} dF_{tan}\,r\,dr \tag{43}$$

$$TSR = \frac{\Omega R}{V_o} \tag{44}$$

in Eqs. (39) and (40), *c* is chord length. dF_{ax} and dF_{tan} are axial and tangential induced forces on the element length in Eqs. (40) and (41) respectively, *R* and r_{hub} are the tip and hub radius of the rotor in Eqs. (43) and (44), *Power* is output power generated by the rotor in Eq. (43) and *TSR* is tip speed ratio of the rotor in Eq. (44).

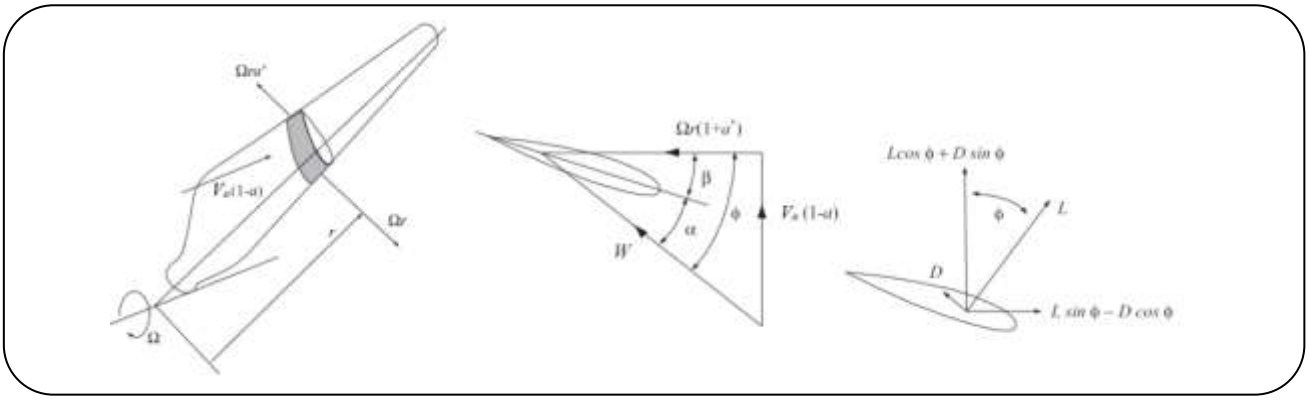

Fig. 3: Arrangement of how to analyze the blade elements.

3D Modeling for the Stall Region

An airfoil data correction described by [53] was used in this study to convert the lift confidence of airfoil data from two dimensions to three dimensions.

$$C_{l,3D} = C_{l,2D} + x\left(\frac{c}{r}\right)^{y} \cos^4(\phi)\left(C_{l,inv} - C_{l,2D}\right) \qquad (45)$$

Finally, as shown in Fig. 4, the following algorithm is used to calculate the output results of BEM.

The wind turbine used in this modeling is a three-bladed horizontal axis and wind turbine with a nominal power output of 150 KW named INER-P150II [54]. The length of each blade is 10.8 meters. The pitch angle and chord length are varied along the wind blade. Also, the airfoil sections used in this wind turbine are DU series, NACA0013166, and FX63-137.

Economic analysis

Economic analysis is one of the most important analyses that is proposed in the field of construction and replacement of a system. Economic analysis is defined as the techniques of comparison, decision-making, and selection through solutions, based on favorable monetary and economic conditions. In general, the use of this analysis is of fundamental importance, because the amount of profit or loss resulting from the quality of the selected method depends on the appropriate use of this technique [55].

Generally, two methods are used to evaluate systems economically. These two methods include static evaluation and dynamic evaluation. Static evaluation is based on criteria that do not include the useful life of the system and the interest rate, but dynamic evaluation includes these two factors [56].

After it becomes clear that the proposed system was technically and environmentally better than traditional systems, economic issues arise. Given that the construction and implementation of an alternative system require the expense of investment, repairs, maintenance, etc., it should be examined whether the revenues and savings of the proposed system will compensate for these costs during its lifetime or not.

To this end, in the economic analysis section of the proposed CHP system, all investment costs, operational costs resulting from the purchase of electricity and fuel, penalties for emissions, repair and maintenance costs, and scrapping are considered and are as follows:

Construction and demolition costs

The cost of building each system includes the initial purchase and investment costs used at the beginning of the system setup. The cost of building a separate production system includes the cost of purchasing a heating boiler and compression chiller. Also in a CHP system, the construction cost includes the initial purchase costs, the backup boiler, and the absorption chiller. The information required to calculate the initial investment cost of simultaneous and separate production system equipment is given in Table 3 [55]. In Table 3, E_{nom} is the initial actuation capacity, H_B is the boiler thermal capacity, C_{nom} is the chiller cooling capacity and C_{wind} is the wind turbine capacity.

Eq. (46) represents the total present value of investment costs at the time of system construction [57].

$$NPWC = \sum_{j=1}^{N}\left(C \times NC\right)_j = 0 \qquad (46)$$

Table. 3 Initial cost of equipment [32,55].

Equipment	The cost of the initial investment (kW/$)
Gas turbine	$C= -0.014E_{nom} + 600$
Boiler	$C= 205\ H_B^{-0.13}$
Compression chiller	$C= 540(C_{nom})^{-0.128}$
Absorption chiller	$C= 482(C_{nom})^{-0.07273} - 159.7$
Wind turbine	$C= 197.5C_{wind}$

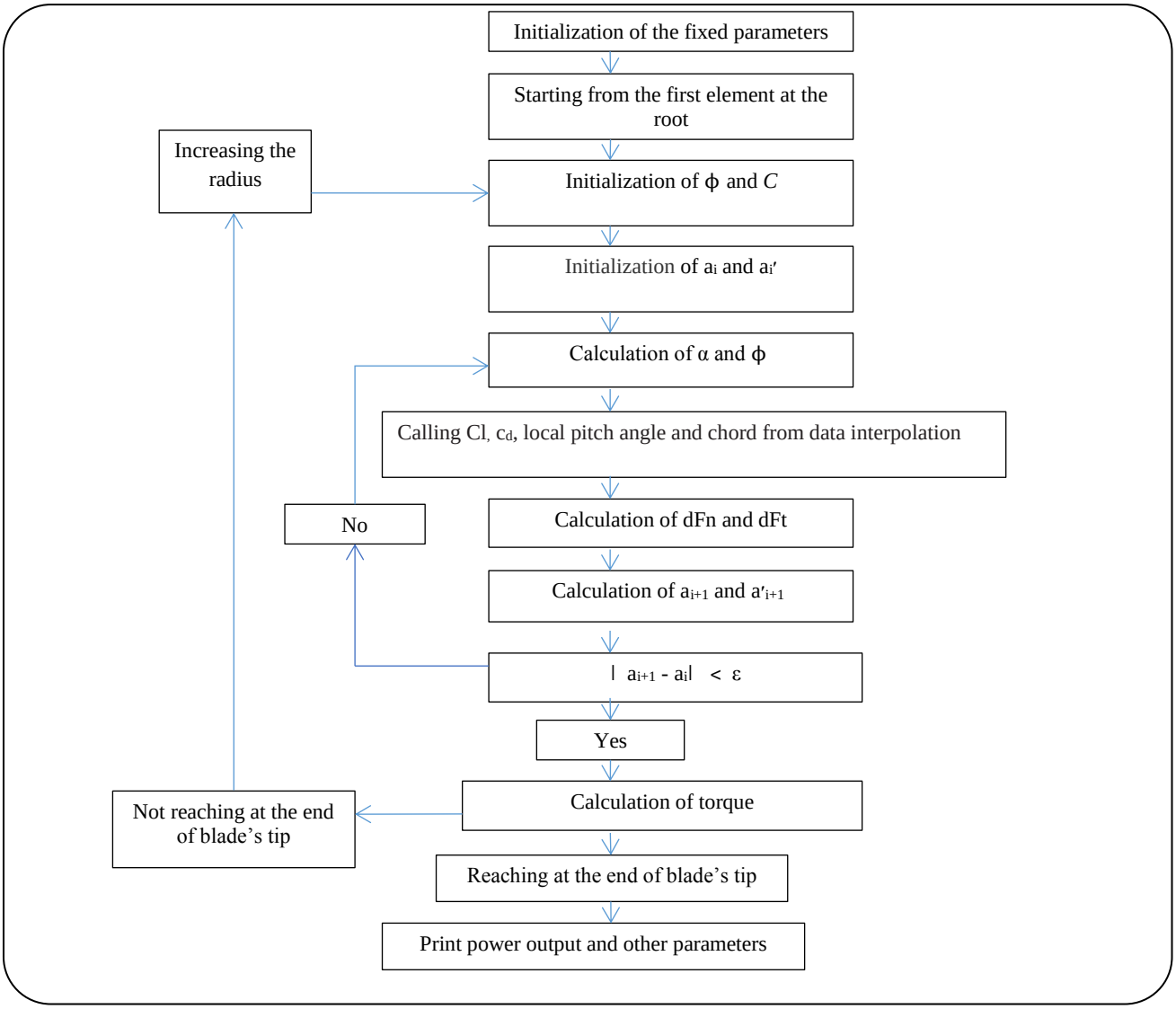

Fig. 4: BEM algorithm used in this study.

In Eq. (46), *NPWC* is the net present value of the initial cost, which is equal to the total cost of purchasing each piece of equipment. Also, *C* is the investment cost per unit capacity of each piece of equipment listed in Table 3. *NC* also shows the rated capacity of each piece of equipment, which is obtained with the help of the relations of the energy analysis section and *J* is also the counter of the equipment.

Also, the cost of constructing the equipment by the equipment (47) is annual [58]:

$$R\beta \times NPWC \quad (47)$$

β is an annualized coefficient and depends on two parameters, the interest rate ***i*** and the system lifetime, *n*. This parameter is evaluated by Eq. (48) [22]:

$$\beta = \frac{i(1-i)^n}{(1-i)^n - 1} \quad (48)$$

A uniform annual cost can be defined by considering the initial cost and the abrupt cost according to Eq. (49). In Eq. (49), *SV* is an annual abortion cost and is obtained from Eq. (50) [24,32,55,59]:

$$EUAC = R - SV \quad (49)$$

$$SV = 0.2 \times NPWC \quad (50)$$

The current value of revenue includes revenue from scrapping costs of *SV* equipment and the annual revenue of the system, which is indicated by *A* and can be assessed by Eq. (51) and (52) [24,55].

$$NPWB = A \times \left[\frac{(1+i)^n - 1}{i(1+i)^n}\right] + SV \times \left[\frac{1}{(1+i)^n}\right] \quad (51)$$

$$A(\$) = \sum_{n=1}^{n}\left[\sum_{t=1}^{8760}\left(E_s \times \mu_{e,s}\right) \times \tau + R_{C\&O\ and\ M}\right] \quad (52)$$

In Eq. (36), $\mu_{e,s}$, the selling price of electricity and $R_{C\&O\ and\ M}$ is the rate of reduction of initial costs, operational costs, reduction of emissions fines, and simultaneous maintenance of the traditional production system. A significant point in these equations is the consideration of interest rates and scrapping costs, which are aligned with the current value method of costs [55].

Maintenance costs

Each equipment requires periodic inspections based on the number of its working hours and, if necessary, replacement or repair of parts. Maintenance costs include basic repairs, replacement of parts such as air filters, oil filters, etc., as well as routine inspections and manpower, which are estimated to be a function of working hours and rated equipment capacity. According to the calculations, the working hours in this study are 5800 hours per year and the lifespan of the equipment is 20 years. The information required to calculate repair and maintenance costs is given in Table 4 [32,55].

Table 4: Cost of equipment repair and maintenance [32,55].

Equipment	Maintenance cost
Gas turbine	M = 0.0055 $/kWh
Boiler	M = 0.0027 $/kWh
Compression chiller	M = 0.003 $/kWh
Absorption chiller	M = 0.003 $/kWh
Wind turbine	M = 0.0021 $/kWh

Methodology

In this study, regarding fig 5, to calculate the overall energy and exergy efficiencies of the CHP system and payback period, firstly, we model the wind turbine based on the BEM theory to calculate the effect of input variables such as inlet velocity, tip speed ratio, and other metrological variables on the system. Then, the first and second thermodynamic laws will be applied to both wind and gas turbines to measure their energy and exergy efficiencies in different conditions. finally, concerning the output power coefficient of the system, economic equations will be used to obtain the payback of the system.

RESULTS AND DISCUSSION

Validation

In this section, before presenting the report, the values and results obtained are first validated. The purpose of the accreditation is to ensure the simulation and its results.

Implementing the BEM method can let us achieve satisfactory anticipation about the power produced in different conditions and calculating the wind speed behind the wind turbine to measure the energy and exergy efficiencies.

Fig 6 shows the comparison between power measurement in real cases and power calculated by BEM code. As is shown, the BEM code has a good ability to predict power production at different wind speeds and pitch angles. Increasing the wind speed from 5 m/s to 12 m/s causes a rise in power production in all three pitch angles, while after peaking at the wind speed of 12 m/s, it has an inverse effect on the power output. On the other hand, increasing the pitch angle decreases power production in all wind speeds. This reduction is more sensible in higher wind speeds. It is predicted that the wind turbine will have the highest performance at the wind speed of 12 m/s and a pitch angle of 5°, which can produce 165 kW power.

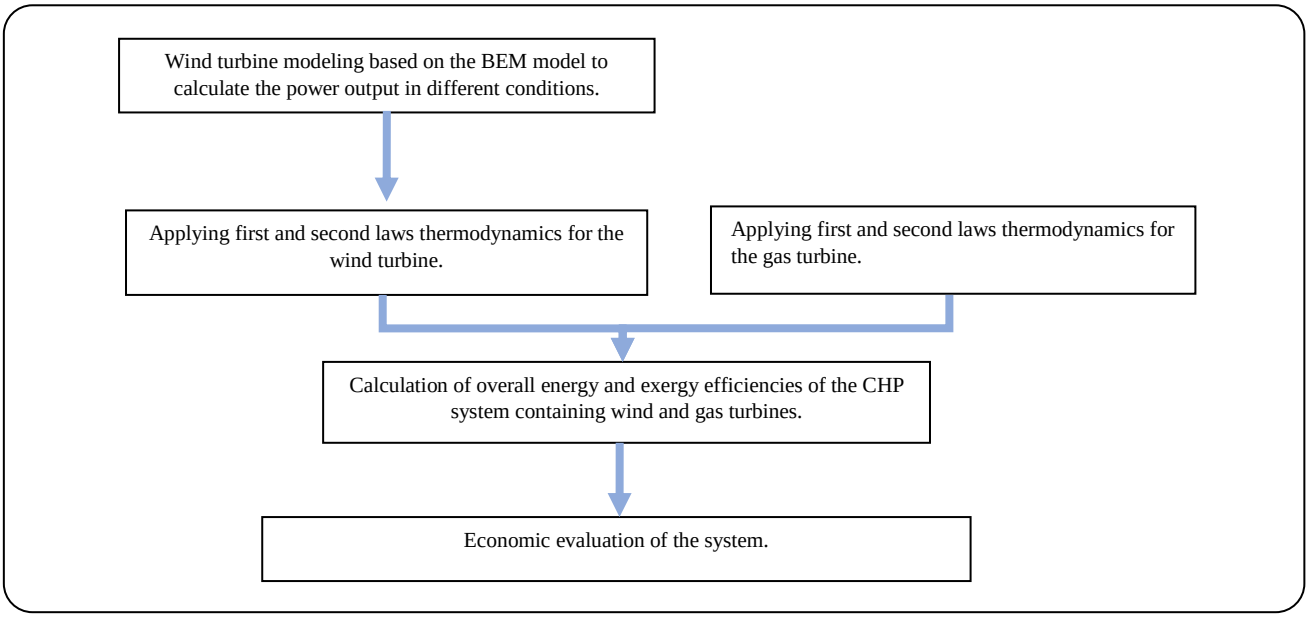

Fig. 5: Overall calculation procedure in this study.

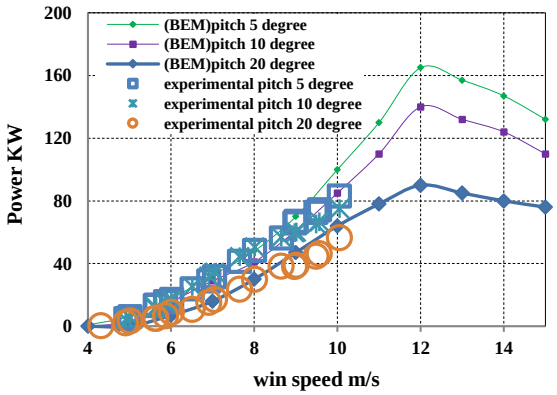

Fig. 6: comparison of output power between BEM model and experimental data.

Wind turbine's energy and exergy analyses

In table 6, as wind speed provides the required kinetic energy to drive the wind turbine, it has a significant effect on the performance of the wind turbine based on both energy and exergy efficiencies. It causes a steady rise in exergy flow and exergy destruction. As wind speed increases, the rate of wake production behind the wind turbine increases, which is the main source of exergy destruction in the turbine. The maximum exergy and energy efficiencies are 42.8 % and 43.9 % at a wind speed 12 m/s and pitch angle 5º.

Another parameter that has a noticeable effect on the energy and exergy efficiencies is Tip Speed Ratio (TSR). Fig 7 shows that increasing the TSR from 1 to 3 increases the energy and exergy efficiencies of the wind turbine for all three wind speeds 8, 10, and 12 m/s, while there is a dramatic reduction in the wind turbine's performance in TSR more than 3 for all three wind speeds. In a fixed wind speed, rotational speed causes a raise in TSR. On the other hand, as the rotational speed is perpendicular to the wind speed direction, it will change the angle of attack on the wind blade, which can help lift coefficient growth. Conversely, in high TSRs, the separation of wind flow on the wind blade increase, which increases the drag coefficient and decreases the lift will of the blade.

Other variables that can affect the wind turbine are the metrological parameters such as pressure changes and the temperature of the wind flow. These effects are shown in Table 7 at the wind speed of 12 m/s and TSR 3. Table 7 shows that increasing the pressure changes can decrease the wind turbine exergy efficiency while increasing the temperature can rise steadily the exergy efficiency from 42.1% at 5ºc to 43% at 35ºc. However, these changes are not noticeable compared to the effect of the TSR and wind speed on the exergy efficiency of the wind turbine.

Overall, it will be assumed that the operating conditions for wind turbines in the system are wind speed 12 m/s, pitch angle 5º, and TSR 3, since the wind turbine has the best performance in these conditions.

Gas turbine results

The parameters examined are the partial load of the prime mover, the pressure ratio, and the combustion chamber temperature.

Table 6: Energy and exergy parameters of the wind turbine in different wind speeds.

Wind speed (m/s)	Energy efficiency (%)	Exergy efficiency (%)	Exergy flow (J)	Exergy destruction (J)
6	14.4	13.16	53175	11464
7	33	30	82449	17337
8	41.7	39.6	121152	23417
9	42.7	41	170619	32088
10	44.56	43.07	232202	42473
11	43.52	42.3	307250	54001
12	43.9	42.8	397105	67889
13	31.2	30.6	503163	70917
14	23.8	23.46	626727	71766
15	17.4	17.1	769150	68426

Table 7: The effect of pressure changes and temperature on the exergy efficiency of wind turbine.

variables	Exergy efficiency (%)
P= 100 Kpa	42.8
P= 150 Kpa	42.6
P= 200 Kpa	42.45
P= 250 Kpa	42.1
T= 5°c	42.4
T= 20°c	42.6
T= 25°c	42.8
T=35°c	43

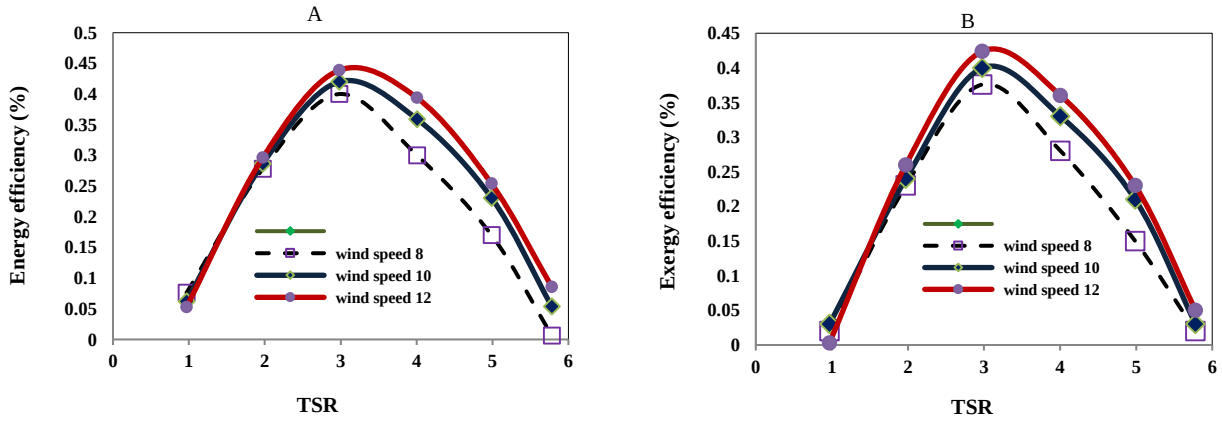

Fig. 7: A) Energy efficiency, B) Exergy efficiency of the wind turbine in different TSR.

The most important parameter affecting the performance of the CHP system is the performance of the prime mover in terms of the partial load. Fig. 7 shows the changes in the ratio of output power and heat received from the prime mover as the two main indicators of the CHP system in terms of partial load for the gas turbine. The horizontal axis shows the percentage of the partial load of the prime mover and the vertical axis also indicates the percentage of fuel consumed.

Fig. 8 shows that input fuel is converted into power and exhaust heat. At different loads, due to the constant inlet and outlet temperature of the combustion chamber and

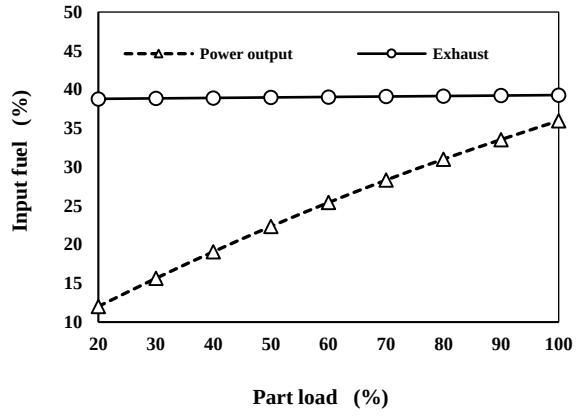

Fig. 8: Technical characteristics of gas turbine in terms of partial load.

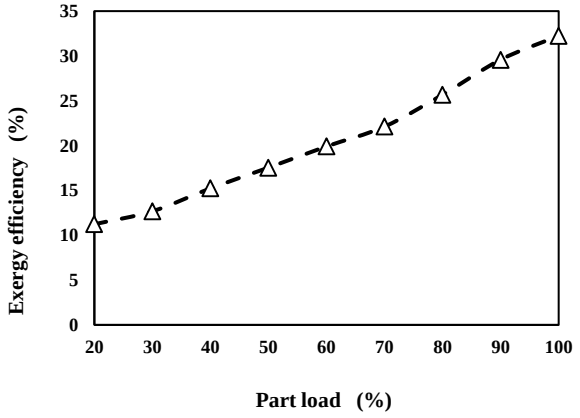

Fig. 9: Exergy efficiency of the gas turbine according to the partial load.

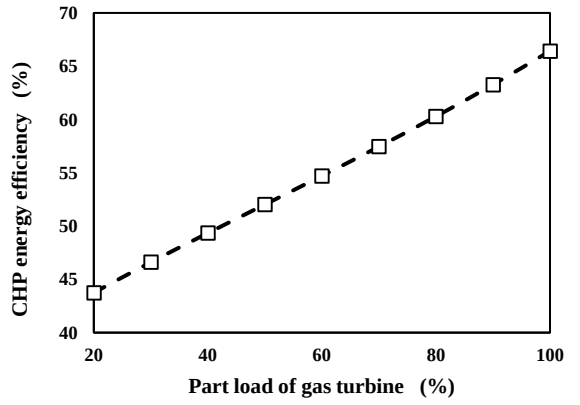

Fig. 10: Diagram of the efficiency of the dual CHP system according to the partial load of the gas turbine.

turbine, the exhaust heat from the exhaust is constant and is shown horizontally. At lower partial loads, a lower percentage of input fuel is converted to power. As the load of the gas turbine increases, a larger percentage of the incoming fuel has turned into power.

According to Fig. 8, it can be assumed that the gas turbine is more suitable for operation at full loads, and for operation, at low loads, it is better to use wind turbines and hybrid systems. Installing two types of generators at the same time can increase fuel efficiency and effectiveness. By installing a lower-capacity gas turbine and several wind turbines, the gas turbine will play its role at full capacity and the rest of the power will be provided by wind turbines.

Fig. 9 shows the exergy efficiency of the according to the partial load of the gas turbine. The exergy efficiency increases with increasing the partial load of the gas turbine and reaches its maximum value at full load. The maximum exergy efficiency cycle introduced at full gas turbine load is about 32%.

The total efficiency of the system

Fig. 10 shows the efficiency of the dual CHP system in terms of the partial load of the gas turbine. The efficiency changes are linear in terms of the partial load of the gas turbine, and the efficiency has increased by about 65% with increasing the load. The minimum efficiency in the combined mode is about 45%, most of which is related to the heat received from the gas turbine exhaust, which can be confirmed by adapting to the previous figure. The reason for the linear change in efficiency is the linear increase in production capacity.

The energy efficiency changes of the dual CHP system in terms of changes in the temperature of the combustion chamber of the gas turbine are shown in fig. 11. At low temperatures, the gas turbine is generally in standby mode and will not produce power, and efficiency has dropped dramatically. By increasing the temperature to 1000°C, the turbine will start and produce power, and the efficiency in this area has increased with a high slope, and these changes have been shown up to 1400°C. Temperatures above 1400°C are not considered due to potential damage to the turbine blades. The best temperature for gas turbines is around 1250°C.

Fig. 12 shows the changes in the energy efficiency of the dual CHP system in terms of the gas turbine pressure ratio.

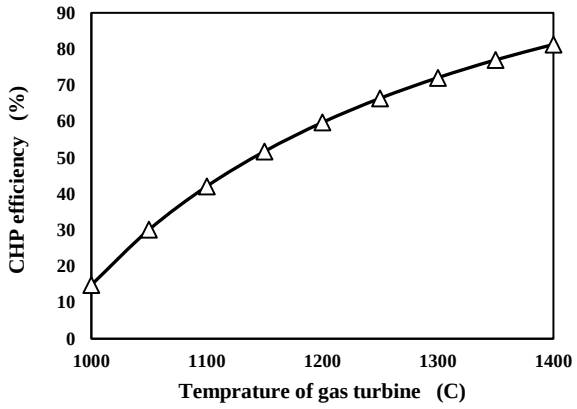

Fig. 11: Chart of changes in the efficiency of the dual CHP system according to the combustion chamber temperature of the gas turbine.

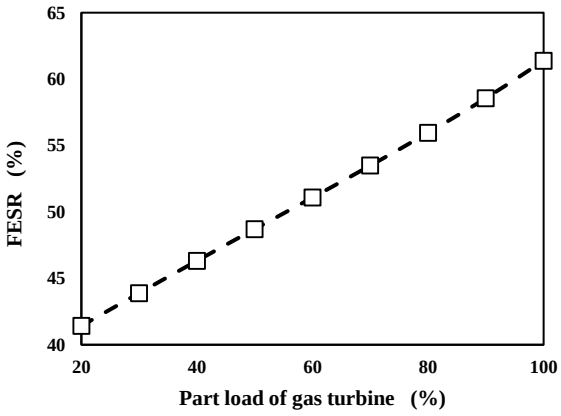

Fig. 13: Chart of fuel consumption changes for dual CHP system in terms of a partial load of the gas turbine.

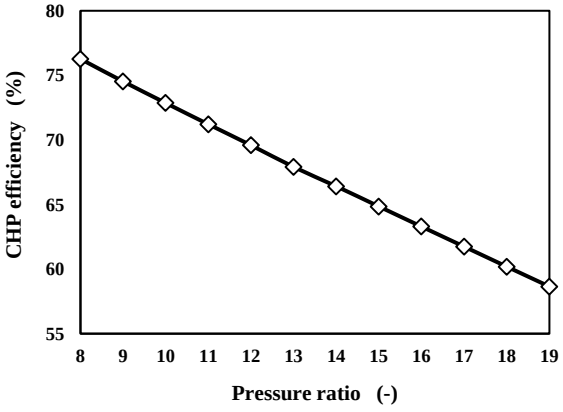

Fig. 12: Chart of change in the efficiency of dual CHP system according to the combustion chamber temperature of the gas turbine.

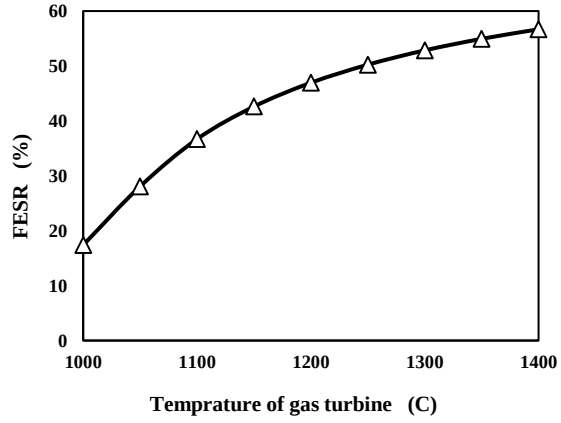

Fig. 14: Chart of fuel consumption changes for dual CHP system according to the temperature of the gas turbine combustion chamber.

The efficiency of the CHP system has decreased when increasing the pressure ratio because it increases the work of the compressor. As a result, the net output and efficiency of the gas turbine will reduce.

Fig. 13 shows the rate of reduction in fuel consumption compared to a separate production system. With increasing partial load, the capacity production of gas turbines has increased, and more fuel has been saved than a separate fuel system. At full load, where power and heat are extracted near the rated load and operating at maximum efficiency, fuel economy savings of more than 50 percent can be seen.

Fig. 14 shows the changes in fuel economy savings of the dual CHP system in terms of changes in the temperature of the gas turbine combustion chamber. As mentioned in the section on efficiency analysis, at low temperatures, the efficiency of the gas turbine is low, and from 1150°C and above, the turbine performs better and saves more on fuel consumption. At higher temperatures, extraction power and heat are increased, and fuel economy savings are higher than in the separate state, which is up to about 50 percent.

Fig. 15 shows a graph of fuel economy savings changes in terms of gas turbine pressure ratio. As the pressure ratio increases, the net output of the gas turbine cycle decreases. As a result, more fuel must be used to increase the production capacity, thus reducing fuel savings, so the slope of the graph is negative.

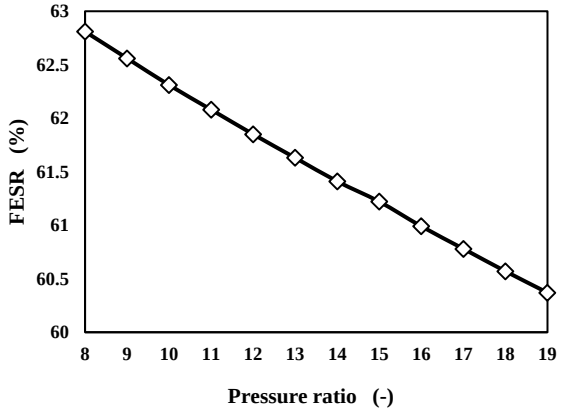

Fig. 15: Chart of fuel energy savings ratio changes for dual CHP system according to gas turbine pressure ratio.

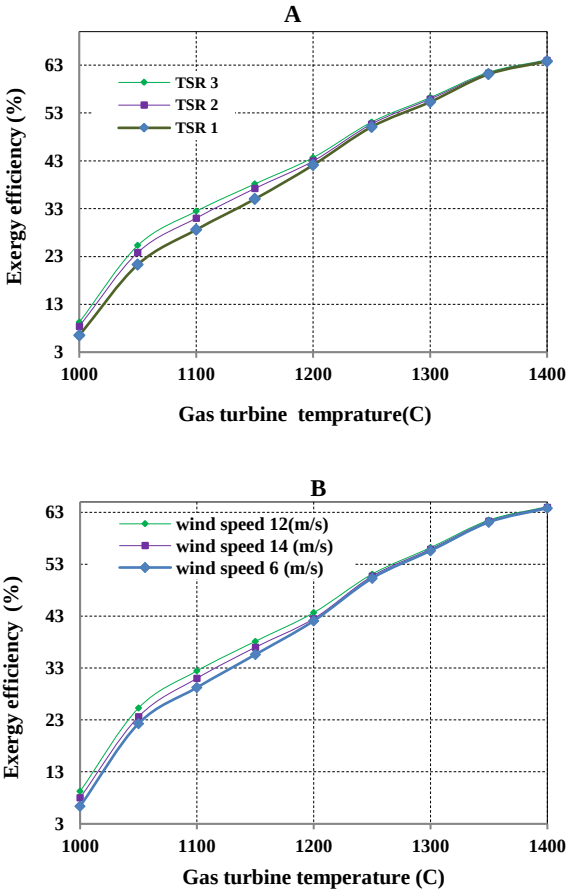

Fig. 16: Effect of A): TSR, B): wind speed on the total Exergy efficiency of the system based on the gas turbine combustion chamber temperature.

Since the gas turbine provides both heat and power and has a high-power capacity as the prime mover, it has the dominant effect on the total performance of the system. However, in figs 16 and 17 the effect of the wind turbine in different TSRs and wind speeds on the exergy efficiency of the total system is investigated. Fig. 16 shows the exergy efficiency of the simultaneous production system introduced according to the temperature changes in the combustion chamber. Generally, increasing the temperature of the combustion chamber rises the exergy efficiency of the system. The reason for this increase in efficiency can be attributed to the increase in work capacity and the differences in environmental dead states. The higher the temperature difference compared to the cold source and the dead conditions of the environment, the greater the ability to perform work and the efficiency of the exergy. As can be seen in fig 16a, this system has the highest performance at TSR 3, which increases from 9.25% at 1000°C to 63.8% at 1400°C. On the other hand, the influence of changing TSR in high temperatures of more than 1200°C is not considerable. It is shown that increasing the TSR from 1 to 3 can increase the total exergy efficiency of the system by 29.7% at the temperature of 1000oC. Also, in fig 16b, the hybrid system has the highest performance at a wind speed 12 m/s. At the temperature of 1000°C, the maximum relative change between wind speeds of 12 m/s and 6 m/s is 22.9%.

In contrast, rising the pressure ratio has decreased the exergy efficiency from 65% at the pressure ratio of 8 to 45.5% at the pressure ratio of 19 and TSR of 3 (see Fig 17a). The system has had the lowest performance at TSR of 1 among the different pressure ratios. The maximum relative change was 6.3% at the pressure ratio of 19 between TSR of 3 and 1, however, this difference at low-pressure ratios is not noticeable. Likewise, the effect of changing wind speed at the high-pressure ratios is more considerable. It can be driven that a wind speed of 6 m/s can decrease the total exergy efficiency of the system by 5% compared to the exergy efficiency of the system at the wind speed of 12 m/s.

Overall, to evaluate the system, it is assumed that the wind turbine is working under the wind speed of 12m/s, the pitch angle of 5^{o} and TSR 3, and the gas turbine is working at the temperature of 1250°C, and the nominal pressure ratio 10.

Fig. 18 shows the payback period in terms of the partial load of the gas turbine. As mentioned,

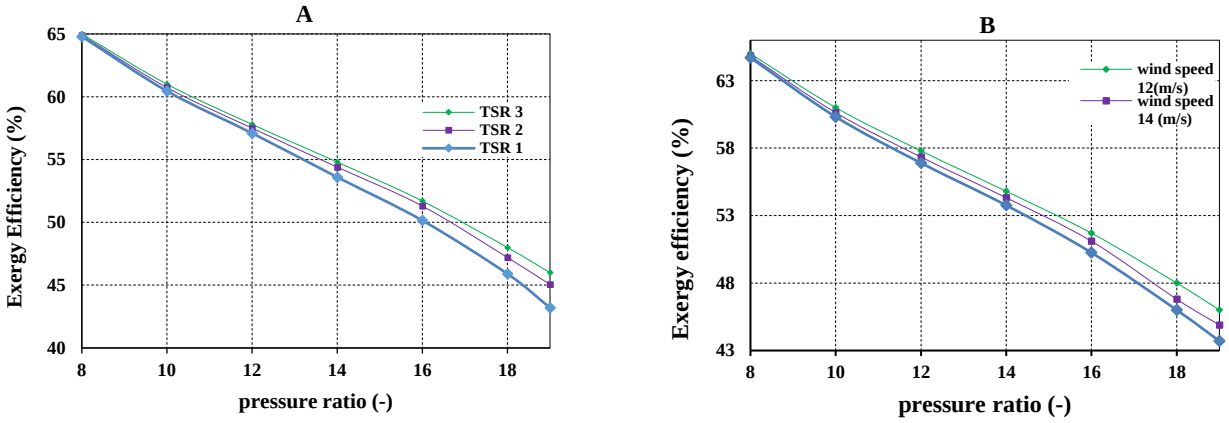

Fig. 17: Effect of A): TSR B): wind speed on the total Exergy efficiency of the system based on the gas turbine pressure ratio.

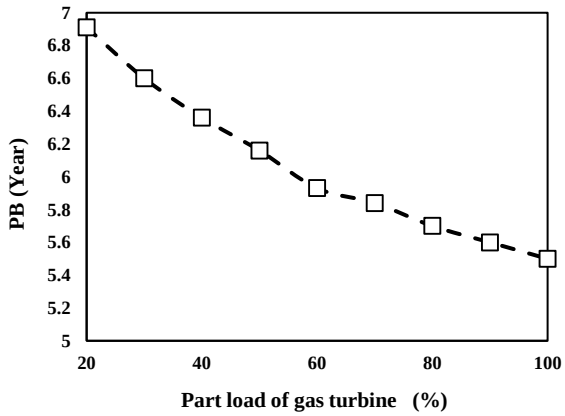

Fig. 18: Chart of the payback period of a dual CHP system in terms of the partial load ratio of the gas turbine.

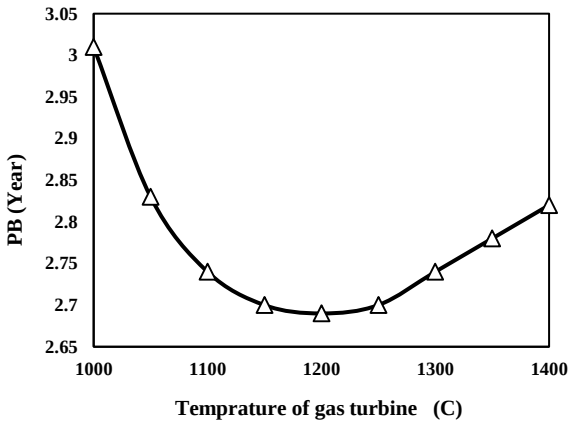

Fig. 19: Chart of the payback period of the dual CHP system according to the temperature of the combustion chamber of the gas turbine.

increasing the partial load improves the performance of the gas turbine, increases efficiency, and saves fuel consumption, thus reducing current costs and reducing the payback period.

Fig. 19 also shows the payback period of the system in terms of combustion chamber temperature. At higher temperatures, due to more damage to the turbine blades, the cost of repairs and maintenance is higher, more fuel is used, and overall increases current costs, thus increasing the payback period.

Fig. 20 shows the payback period according to the gas turbine pressure ratio. Increasing the gas turbine pressure ratio increases the work of the compressor and reduces the net output, thus delaying and increasing the payback period. Because labor and temperature changes are relative to pressure, changes in cost and payback period will also be contributory, and there will be more changes in the ratio of high pressures.

CONCLUSIONS

The results show that the use of gas turbines and wind turbines as the prime movers of the CHP system will increase efficiency, the savings on primary fuel consumption, and reduce operational costs.

The highest energy and exergy efficiencies for wind turbines are obtained at wind speeds of 12 m/s and TSR of 3.

Compared to wind speed and TSR, the effect of changes in air pressure and ambient temperature on the exergy efficiency of the wind turbine and the CHP system is not significant.

Increasing the gas turbine pressure ratio reduces the overall exergy efficiency of the CHP system. On the other hand, by this reduction, the overall behavior of the system will be affected by wind speed and the wind turbine TSR. As a result, it is better for the gas turbine to operate at a pressure ratio of 10 to reduce fluctuations in system energy and exergy efficiencies.

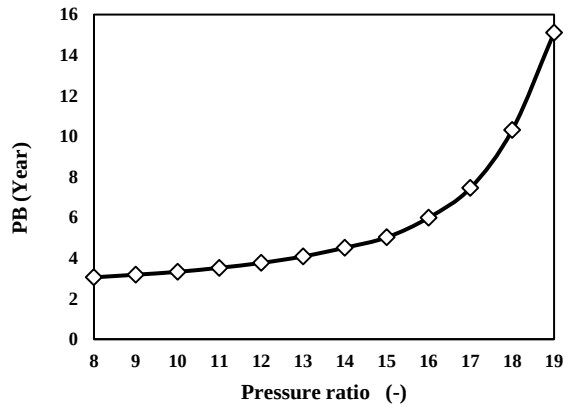

Fig. 20: Chart of the payback period of dual CHP system according to gas turbine pressure ratio.

Changing the combustion chamber temperature improves cycle efficiency to some extent, but it causes increases in fuel consumption, operating costs, and payback periods at high temperatures. On the other hand, since the wind turbine can change the overall efficiency at a combustion chamber temperature below 1250 °C, working at the temperature of 1250 °C can provide a stable efficiency for the system.

Nomenclature

a	Axial induction factor
a'	Tangential induction factor
C	Chord
Cl	Lift coefficient
Cd	Drag coefficient
CC	Capital Cost
CHP	Combined Heating and Power
CCHP	Combined Cooling, Heating and Power
Cp	Heat confidence
CR	Cost reduction
D	Drag force
E	Energy
F	Fuel & Force
FESR	Fuel energy saving ratio
H	Heat Load
h	Enthalpy
i	Interest rate
Ke	Kinetic energy
L	Lift force
LHV	Low heating value
m	Mass flow
M	Maintenance
n	Lifetime of the equipment
NPWB	Net present worth benefit
NPWC	Net present worth cost
P	Power load & pressure
PB	Payback Period
PL	Part Load
PM	Prime Mover
Q	Heat transfer rate
R	Reduce costs & Radius
SHP	Separate Production
SV	Salvage value
TSR	Tip speed ratio
V	Velocity
W	Work

Subscript

cp	Power coefficient
f	Prandtl's tip loss factor
in	Inlet flow
nom	Nominal
out	Outlet flow
rec	Recovery
req	Request
y	Year

Greek symbols

α	Angle of attack, rad
β	Pitch angle, rad
η	Energy efficiency
Ω	Rotor speed, rad/s
ρ	Density, kg/m^3
σ'	Solidity
φ	Flow angle, rad
Ψ	Exergy efficiency

Received : Feb. 16, 2021 ; Accepted : Aug. 2, 2021

REFERENCES

[1] Ahmadi M.H., Ahmadi M.A., Bayat R., Ashouri M., Feidt M., Thermo-Economic Optimization of Stirling Heat Pump by Using Non-Dominated Sorting Genetic Algorithm, *Energy Convers. Manag.*, **91**: 315–322 (2015). https://doi.org/10.1016/j.enconman.2014.12.006.

[2] Naseri A., Bidi M., Ahmadi M.H., Thermodynamic and Exergy Analysis of a Hydrogen and Permeate Water Production Process by a Solar-Driven Transcritical CO_2 Power Cycle with Liquefied Natural Gas Heat Sink, *Renew. Energy*., **113**: 1215–1228 (2017). https://doi.org/10.1016/j.renene.2017.06.082.

[3] Javadi M.A., Hoseinzadeh S., Ghasemiasl R., Heyns P.S., Chamkha A.J., Sensitivity Analysis of Combined Cycle Parameters on Exergy, Economic, and Environmental of a Power Plant, *J. Therm. Anal. Calorim.*, **139**: 519–525 (2020). https://doi.org/10.1007/s10973-019-08399-y.

[4] Caruso C., Catenacci G., Marchettini N., Principi I., Tiezzi E., Emergy Based Analysis Of Italian Electricity Production System, *J. Therm. Anal. Calorim.*, 265–272 (2001). https://doi.org/10.1023/A:1012412420744.

[5] Naeimi A., Bidi M., Ahmadi M.H., Kumar R., Sadeghzadeh M., Alhuyi Nazari M., Design and Exergy Analysis of Waste Heat Recovery System and Gas Engine for Power Generation in Tehran Cement Factory, *Therm. Sci. Eng. Prog.*, **9**: 299–307 (2019). https://doi.org/10.1016/j.tsep.2018.12.007.

[6] Ahmadi M.H., Ghazvini M., Sadeghzadeh M., Alhuyi Nazari M., Ghalandari M., Utilization of Hybrid Nanofluids in Solar Energy Applications: A Review, *Nano-Structures and Nano-Objects.*, **20**: 100386 (2019). https://doi.org/10.1016/j.nanoso.2019.100386.

[7] Ansarinasab H., Mehrpooya M., Sadeghzadeh M., An Exergy-Based Investigation on Hydrogen Liquefaction Plant-Exergy, Exergoeconomic, and Exergoenvironmental Analyses, *J. Clean. Prod.*, **210**: 530–541 (2019). https://doi.org/10.1016/j.jclepro.2018.11.090.

[8] Ahmadi M.H., Mehrpooya M., Pourfayaz F., Thermodynamic and Exergy Analysis and Optimization of a Transcritical CO_2 Power Cycle Driven by Geothermal Energy with Liquefied Natural Gas as its Heat Sink, *Appl. Therm. Eng.*, **109**: 640–652 (2016). https://doi.org/10.1016/j.applthermaleng.2016.08.141.

[9] Naseri A., Bidi M., Ahmadi M.H., Saidur R., Exergy Analysis of a Hydrogen and Water Production Process by a Solar-Driven Transcritical CO_2 Power Cycle with Stirling Engine, *J. Clean. Prod.*, **158**: 165–181 (2017). https://doi.org/10.1016/j.jclepro.2017.05.005.

[10] Nouri M., Namar M.M., Jahanian O., Analysis of a developed Brayton Cycled CHP System Using ORC and CAES Based on First and Second Law of Thermodynamics, *J. Therm. Anal. Calorim.*, **135**: 1743–1752 (2019). https://doi.org/10.1007/s10973-018-7316-6.

[11] Jamalabadi M.Y.A., Carbon Monoxide Reduction in Solid Oxide Fuel Cell–Mini Gas Turbine Hybrid Power System, *J. Therm. Anal. Calorim.*, **135**: 1871–1880 (2019). https://doi.org/10.1007/s10973-018-7513-3.

[12] Jamalabadi M.Y.A., Numerical Simulation of Carbon Dioxide Sorption Circulating Fluidized Bed Used in Solid Oxide Fuel Cell, *J. Therm. Anal. Calorim.*, **139**: 2565–2575 (2020). https://doi.org/10.1007/s10973-019-08565-2.

[13] Bagherzadeh S.A., Ruhani B., Namar M.M., Alamian R., Rostami S., Compression Ratio Energy and Exergy Analysis of a Developed Brayton-Based Power Cycle Employing CAES and ORC, *J. Therm. Anal. Calorim.*, **139**: 2781–2790 (2020). https://doi.org/10.1007/s10973-019-09051-5.

[14] Senturk Acar M., Arslan O., Energy and Exergy Analysis of Solar Energy-Integrated, Geothermal Energy-Powered Organic Rankine Cycle, *J. Therm. Anal. Calorim.*, **137**: 659–666 (2019). https://doi.org/10.1007/s10973-018-7977-1.

[15] Ahmadi M.H., Alhuyi Nazari M., Sadeghzadeh M., Pourfayaz F., Ghazvini M., Ming T., Meyer J.P., Sharifpur M., Thermodynamic and Economic Analysis of Performance Evaluation of All the Thermal Power Plants: A Review, *Energy Sci. Eng.*, **7**: 30–65 (2019). https://doi.org/10.1002/ese3.223.

[16] (5) Use of bioethanol in a Gas turbine Combustor | Request PDF, (n.d.). https://www.researchgate.net/publication/269940196_Use_of_bioethanol_in_a_gas_turbine_combustor (accessed April 20, 2020).

[17] Cavarzere A., Morini M., Pinelli M., Spina P.R., Vaccari A., Venturini M., Experimental Analysis of a Micro Gas Turbine Fuelled with Vegetable Oils from Energy Crops, *in: Energy Procedia*, Elsevier, pp. 91–100 (2014). https://doi.org/10.1016/j.egypro.2014.01.011.

[18] Yucer C.T., Thermodynamic Analysis of the Part Load Performance for a Small Scale Gas Turbine Jet Engine by Using Exergy Analysis Method, *Energy*, **111**: 251–259 (2016). https://doi.org/10.1016/j.energy.2016.05.108.

[19] Kaushik S.C., Singh O.K., Estimation of Chemical Exergy of Solid, Liquid and Gaseous Fuels Used in Thermal Power Plants, *J. Therm. Anal. Calorim.*, **115**: 903–908 (2014). https://doi.org/10.1007/s10973-013-3323-9.

[20] Namar M.M., Jahanian O., Energy and Exergy Analysis of a Hydrogen-Fueled HCCI Engine, *J. Therm. Anal. Calorim.*, **137**: 205–215 (2019). https://doi.org/10.1007/s10973-018-7910-7.

[21] Kalbasi R., Izadi F., Talebizadehsardari P., Improving Performance of AHU Using Exhaust Air Potential by Applying Exergy Analysis, *J. Therm. Anal. Calorim.*, **139**: 2913–2923 (2020). https://doi.org/10.1007/s10973-019-09198-1.

[22] Mohammadi A., Kasaeian A., Pourfayaz F., Ahmadi M.H., Thermodynamic Analysis of a Combined Gas Turbine, ORC Cycle and Absorption Refrigeration for a CCHP System, *Appl. Therm. Eng.*, **111**: 397–406 (2017). https://doi.org/10.1016/j.applthermaleng.2016.09.098.

[23] Ahmadi M.H., Sayyaadi H., Mohammadi A.H., Barranco-Jimenez M.A., Thermo-Economic Multi-Objective Optimization of Solar Dish-Stirling Engine by Implementing Evolutionary Algorithm, *Energy Convers. Manag.*, **73**: 370–380 (2013). https://doi.org/10.1016/j.enconman.2013.05.031.

[24] Kim S., Lee S., Ryu J., Spitsyn V.E., "Development of the 5MW Power Generation Gas Turbine Engine", in: *Proc. ASME Turbo Expo*, American Society of Mechanical Engineers Digital Collection, pp. 591–598 (2011). https://doi.org/10.1115/GT2011-45778.

[25] Khanjari A., Mahmoodi E., Ahmadi M.H., Energy and Exergy Analyzing of a Wind Turbine in Free Stream and Wind Tunnel In CFD Domain Based on Actuator Disc Technique, *Renew. Energy*. (2020). https://doi.org/10.1016/j.renene.2020.05.183.

[26] Khanjari A., Mahmoodi E., Sarreshtehdari A., Chahartaghi M., Modelling of Energy and Exergy Efficiencies of a Horizontal Axis Wind Turbine Based on the Blade Element Momentum Theory at Different Yaw Angles, *Int. J. Exergy.*, **27**: 437–459 (2018). https://doi.org/10.1504/IJEX.2018.096002.

[27] e. a. C. o. C. t. W. Darrow K, No Title, US Environ. Prot. Agency, 5–6 (2015).

[28] Li Q., Kamada Y., Maeda T., Murata J., Yusuke N., Effect of Turbulence on Power Performance of a Horizontal Axis Wind Turbine In Yawed and No-Yawed Flow Conditions, *Energy*, **109**: 703–711 (2016). https://doi.org/10.1016/j.energy.2016.05.078.

[29] Ebrahimi M., The Environ-Thermo-Economical Potentials of Operating Gas Turbines in Industry for Combined Cooling, Heating, Power and Process (CCHPP), *J. Clean. Prod.*, **142**: 4258–4269 (2017). https://doi.org/10.1016/j.jclepro.2016.12.001.

[30] Korlu M., Pirkandi J., Maroufi A., Thermodynamic Analysis of a Gas Turbine Cycle Equipped with a Non-Ideal Adiabatic Model for a Double Acting Stirling Engine, *Energy Convers. Manag.*, **147**: 120–134 (2017). https://doi.org/10.1016/j.enconman.2017.04.049.

[31] Caresana F., Pelagalli L., Comodi G., Renzi M., Microturbogas Cogeneration Systems for Distributed Generation: Effects of Ambient Temperature on Global Performance and Components' Behavior, *Appl. Energy.*, **124**: 17–27 (2014). https://doi.org/10.1016/j.apenergy.2014.02.075.

[32] Sanaye S., Meybodi M.A., Shokrollahi S., Selecting the Prime Movers and Nominal Powers In Combined Heat and Power Systems, *Appl. Therm. Eng.*, **28**: 1177–1188 (2008). https://doi.org/10.1016/j.applthermaleng.2007.08.003.

[33] Espirito Santo D.B., Energy and Exergy Efficiency of a Building Internal Combustion Engine Trigeneration System Under Two Different Operational Strategies, *Energy Build*, **53**: 28–38 (2012). https://doi.org/10.1016/j.enbuild.2012.06.014.

[34] Al-Sulaiman F.A., Hamdullahpur F., Dincer I., Greenhouse Gas Emission and Exergy Assessments of an Integrated Organic Rankine Cycle with a Biomass Combustor for Combined Cooling, Heating and Power Production, *Appl. Therm. Eng.*, **31**: 439–446 (2011). https://doi.org/10.1016/j.applthermaleng.2010.09.019.

[35] Gungor A., Erbay Z., Hepbasli A., Gunerhan H., Splitting the Exergy Destruction into Avoidable and Unavoidable Parts of a Gas Engine Heat Pump (GEHP) for Food Drying Processes Based on Experimental Values, *Energy Convers. Manag.*, **73**: 309–316 (2013). https://doi.org/10.1016/j.enconman.2013.04.033.

[36] Khaliq A., Dincer I., Energetic and Exergetic Performance Analyses of a Combined Heat and Power Plant with Absorption Inlet Cooling and Evaporative Aftercooling, *Energy*, **36**: 2662–2670 (2011). https://doi.org/10.1016/j.energy.2011.02.007.

[37] J.G. Speight, A Review of: "The Exergy Method: Technical and Ecological Applications," Energy Sources. 27 (2005) 1099–1101. https://doi.org/10.1080/00908310500214958.

[38] Chahartaghi M., Kharkeshi B.A., Performance Analysis of a Combined Cooling, Heating and Power System with PEM Fuel Cell as a Prime Mover, *Appl. Therm. Eng.*, **128**: 805–817 (2018). https://doi.org/10.1016/j.applthermaleng.2017.09.072.

[39] Ahmadi M.H., Ahmadi M.A., Mellit A., Pourfayaz F., Feidt M., Thermodynamic Analysis and Multi Objective Optimization of Performance of Solar Dish Stirling Engine by the Centrality of Entransy and Entropy Generation, *Int. J. Electr. Power Energy Syst.*, **78**: 88–95 (2016). https://doi.org/10.1016/j.ijepes.2015.11.042.

[40] The Exergy Method of Thermal Plant Analysis, Elsevier, (1985). https://doi.org/10.1016/c2013-0-00894-8.

[41] Bluestein M., Zecher J., A New Approach to an Accurate Wind Chill Factor, *Bull. Am. Meteorol. Soc.*, **80**: 1893–1899 (1999). http://journals.ametsoc.org/doi/abs/10.1175/1520-0477(1999)080%3C1893:ANATAA%3E2.0.CO;2

[42] Boojari M., Mahmoodi E., Khanjari A., Wake Modelling Via Actuator-Line Method for Exergy Analysis in Open FOAM, *Int. J. Green Energy.*, **16**: 797–810 (2019). https://doi.org/10.1080/15435075.2019.1641101.

[43] Mahmoodi E., Schaffarczyk A.P., "Actuator Disc Modeling of the MEXICO Rotor Experiment", Springer Berlin Heidelberg, pp. 29–34 (2014). https://doi.org/10.1007/978-3-642-54696-9_5.

[44] Song Y., Perot J.B., CFD Simulation of the NREL Phase VI Rotor, *Wind Eng.*, 39 (2015). https://doi.org/10.1260/0309-524X.39.3.321.

[45] Khanjari A., Sarreshtehdari A., Mahmoodi E., Modeling of Energy and Exergy Efficiencies of a Wind Turbine Based on the Blade Element Momentum Theory Under Different Roughness Intensities, *J. Energy Resour. Technol.*, **139**: 022006 (2016). https://doi.org/10.1115/1.4034640.

[46] Khanjari A., Mahmoodi E., Sarreshtehdari A., Effect of Stall Delay Model on Momentum Distribution of Wind Turbine's Blade under Yaw Condition: Compared to MEXICO Experiment, *Iranica Journal of Energy & Environment*, **9**: 16–23 (2018). https://doi.org/10.5829/ijee.2018.09.01.03.

[47] Martin O.L. Hansen, "Aerodynamics of Wind Turbines", 2nd ed., (2008). https://doi.org/10.1002/0470846127.

[48] Glauert H., "Airplane Propellers", Division L. Julius Springer, New York, (1935).

[49] Mahmoodi E., Jafari A., Peter Schaffarczyk A., Keyhani A., Mahmoudi J., A New Correlation on the MEXICO Experiment Using a 3D Enhanced Blade Element Momentum Technique, *Int. J. Sustain. Energy.*, 1–13 (2013). https://doi.org/10.1080/14786451.2012.759575.

[50] Wilson R., Fundamental Concepts in Wind Turbine Engineering, in: Spera, D.A, 2 ed, ASME, New York, 2009. (accessed December 22, 2015).

[51] Hernandez J., Crespo A., Aerodynamics Calculation Of the Performance of Horizontal Axis Wind Turbines and Comparison with Experimental Results, *Wind Eng.*, **11**: 177–187 (1987).

[52] Moriarty P., Hansen A., AeroDyn Theory Manual, National Renewable Energy Laboratory, colorado, (2005).

[53] Chaviaropoulos D.P.K., Dr., Head of the Research and Development Department and M. O. L. Hansen, Investigating Three-Dimensional and Rotational Effects on Wind Turbine Blades by Means of a Quasi-3D Navier-Stokes Solver, *J. Fluids Eng.*, **122**: 330–336 (2000).

[54] Lin Y.T., Chiu P.H., Huang C.C., An Experimental and Numerical Investigation on the Power Performance of 150 kW Horizontal Axis Wind Turbine, *Renew. Energy.*, **113**: 85–93 (2017). https://doi.org/10.1016/j.renene.2017.05.065.

[55] Tavakoli Dastjerd F., Ghafuoryan M.M., Shakib S.E., Tech Economic Optimization of CCHP System with Rely the Time Value of Money, in Payback Period, *Modares Mech. Eng.*, **99**: 254–260 (2015) *[In Persian]*.

[56] Gu Q., Ren H., Gao W., Ren J., Integrated Assessment of Combined Cooling Heating and Power Systems under Different Design and Management Options for Residential Buildings in Shanghai, *Energy Build*, **51**: 143–152 (2012). https://doi.org/10.1016/j.enbuild.2012.04.023.

[57] Sanaye S., Ghafurian M.M., Applying Relative Equivalent Uniform Annual Benefit for Optimum Selection of a Gas Engine Combined Cooling, Heating and Power System for Residential Buildings, *Energy Build*, **128**: 809–818 (2016). https://doi.org/10.1016/j.enbuild.2016.07.015.

[58] Tavakoli Dastjerd F., Ghafuoryan M.M., Shakib S.E., Comparison of Selection Effect Environmental Optimization and Multi-Criteria Optimizations, *Energy, Econ. Environ. Perform. CCHP Syst.* 69–77 (2015). [In Persain],

[59] Ebrahimi M., Keshavarz A., Sizing the Prime Mover of a Residential Micro-Combined Cooling Heating and Power (CCHP) System by Multi-Criteria Sizing Method for Different Climates, *Energy*, **54**: 291–301 (2013). https://doi.org/10.1016/j.energy.2013.01.061.